EXECUTIVE SUMMARY

Title: Synthesis and characterization of Inorganic Semiconductor Nanoparticles and their applications.

Executive summary of a thesis submitted to

The Maharaja Sayajirao University of Baroda,

For the degree of

Doctor of Philosophy

In

Chemistry

Submitted by

NeelamKumari Gupta

Under The Guidance Of

Dr. Hemant P Soni

Chemistry Department,

Faculty of Science

The Maharaja Sayajirao University of Baroda.

Vadodara 390002,

Gujarat India

2022

Synthesis and characterization of Inorganic semiconductor nanoparticles and their applications

Thesis entitled Synthesis and characterization of Inorganic Semiconductor Nanoparticles and their applications. This thesis outlines the work of two discrete projects. Chapter 1 includes a brief introduction to semiconductor nanoparticles, and Chapters 2 to 3 detail the study of faceted nanoparticles and their comparative catalytic activity towards the C-H bond selective functionalizing. Chapters 4 to 5 detail the study of mono-doped, dual-doped heterogeneous catalytic system and their efficiency towards dye degradation.

The specific objective of this study is to examine the role of heterogeneous catalysts in the Direct oxidation of benzylic sp^3 C−H to the corresponding carbonyl, for that purpose developing a mild, efficient, and environmentally friendly method that uses simple reagents/oxidants (e.g., O_2 gas) for benzylic C−H oxidation. The study was continued for the Heterogeneous photo-catalytic system using metal sulfide (mono-doped and dual-doped) semiconductor NPS as an effective technology for wastewater treatment.

The thesis employed an experimental approach designed in different stages: selection of catalyst, the purpose of catalyst for the chosen, synthesis of catalyst, characterization of catalyst by different spectroscopic techniques, catalytic applications, conclusions, bibliography, and webliography.

The table of contents:

Chapter 1: Introduction of semiconductor NPS

It is a general introduction to semiconductor Nps, and their synthesis methods including (1) Bottom-up Method and (2) Top-down method including advantages and disadvantages, and classifications, classified based on the number of dimensions, zero-dimensional (including quantum dots, Nanospheres, hollow spheres falls in this category) one-dimensional (including Nanorods, nanotubes, nanowires), two-dimensional (including Nanofilms, Nanocoatings), three-dimensions (includes Carbon-based nano-materials, Metal-based nano-materials, Dendrimers Composite) and applications in different areas are discussed. Semiconductor NPS have at least one dimension is less than 100 nm, possess properties between metals and non-metals, have a High Surface area, are highly chemically reactive, have wide bandgaps, and therefore allow significant alteration in their properties with bandgap tuning. Hence semiconductor NPS performed an excellent catalytic activity.

Chapter 2: Benzylic Csp^3-H Bond Oxidation on (111) Facets of *o*-Cu_2O Nanocrystals: C-H Bond Activation through Semiconductor Facets Mediated Catalysis.

Methodology:

In this study octahedral-shaped Cu_2O nanocrystals (*o*-Cu_2O NCs) have been synthesized by the wet chemical method. For that, 6.0 mmol of cupric acetate ($Cu(CH_3COO)_2.H_2O$) and 0.12 mmol (in repeating unit) of polyvinyl alcohol (PVA) were dissolved in 50.0 mL water at 60 ^oC. First, Then, the aqueous solution of NaOH (120 mmol, 4.8g in 20.0 mL) was added dropwise under vigorous stirring. Then 20.0 mL aqueous solution of ascorbic acid (18.0 mmol) was added quickly to the above suspension under vigorous stirring, and a reddish color was obtained after 30 min of stirring. The reaction mixture was centrifuged at 6000 rpm for 10 min. The collected product was washed with DI water (5 times) and finally with absolute alcohol and dried in hot air oven at 60 ^oC. As Synthesized Cu_2O nanocrystals characterized by powder X-ray diffraction (PXRD), X-ray Photoelectron Spectroscopy (XPS), Field-Emission Scanning Electron Microscopy (FESEM), and High-Resolution Transmission Electron Microscopy (HRTEM), it was confirmed that the synthesized material was Cu_2O NCs with octahedral morphology with the (111) facets exposed. The synthesized *o*-Cu_2O NCs have been explored as the catalyst for benzylic sp^3 C-H bond oxidation. Reaction parameters like oxidants, solvents, temperature, and reaction time were optimized for the model oxidation reaction involving diphenylmethane (DPM) as a substrate. For that 0.166 mL diphenylmethane (1.0 mmol) was dissolved in 6.0 mL acetonitrile in 10.0 mL round bottom flask and stirred for 5 min. *o*-Cu_2O NCs (3.5 mol%) were subsequently added and the mixture was stirred for 10 min. Finally, 0.52 mL t-butyl hydroperoxide (TBHP, 4.0 mmol) was added, and the reaction mixture was stirred for 6 days at RT. The reaction progress was monitored on the TLC plate every 4 h (for optimization of reaction parameters). After completing the reaction (96 h), the reaction mixture was centrifuged to recover the catalyst; the excess of TBHP was destroyed by adding excess sodium metabisulphite into the reaction mixture. The excess reagents were distilled out. The product was extracted with ethyl acetate and dried over sodium sulfate. The crude product was purified by column chromatography using petroleum ether (60-80 ^{o}C) as eluent. The product obtained was analyzed by ^{1}H-NMR.

Conclusion

The results obtained indicate that the substrate having a benzylic sp^3 C-H bond can be easily oxidized to a corresponding carbonyl compound in the presence of these nanocrystals at RT by stirring the reaction mixture over the bar magnet (up to 92% conversion). The oxidation of Cu_2O to CuO occurs all together with the progress of the reaction when carried out under a typical aerial atmosphere in the presence of light (daylight and mercury CFL tubes prevailing in the laboratory). However, this can be avoided when the reaction was carried out in a dark or inert atmosphere or continuous flow of oxygen gas. BET surface area analysis was carried out to confirm the catalytic effect due to facets. The experimental results lead to proving the activation of O_2 molecules through the Single Electron Transfer (SET) mechanism on the (111) facets of semiconducting Cu_2O NCs in light.

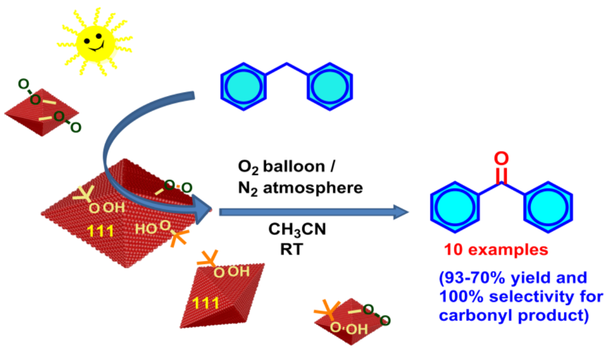

Cu_2O (111) facets for Benzylic C_{sp^3}-H bond Oxidation

(From the optimization of oxidation of DPM as model reaction, free radical scavenger experiments and special experiments, following conclusions can be drawn: (1) Cu^{1+} ended (111) facets of o-Cu_2O NCs are capable to activate oxygen molecules to undergo reduction by SET mechanism in presence of light, and the in situ generated superoxo species immediately abstract the ·H radical from the nearby substrate and initiate the cascade of chemical reactions and electronic processes resulting into stable oxidation product and complete restructuring of the crystal lattice of the catalyst, respectively (2) The etching of the (111) surfaces during the oxidation process can be avoided if the reaction is carried out in dark or under inert atmosphere or under continuous flow of oxygen gas (3) The developed protocol for benzylic sp^3C-H bond oxidation to ketone is applicable under mild conditions with complete selectivity just by stirring the reaction mixture over bar magnet for 4 days (4)

Suggestions/Recommendations

(111) faceted Cu_2O nanocrystals having octahedral morphology can be synthesized. The exposed (111) facets of Cu_2O NCs can be explored as catalytic sites for the benzylic sp^3C-H bond oxidation process. This protocol is equally and effectively applied to a wide range of substrates having C-H bond energy less than 90 kcal/mol. The (111) facets of *o*-Cu_2O NCs can be regenerated for the successive three catalytic cycles with minute loss in reactivity by maintaining the proper reaction conditions.

Bibliography/webliography

1. Hartwig, J. F. Evolution of C−H Bond Functionalization from Methane to Methodology. J. Am. Chem. Soc. 2016, 138, 2−24.
2. Gensch, T.; Hopkinson, M. N.; Glorius, F.; Wencel-Delord, J. Mild Metal-Catalyzed C−H Activation: Examples and Concepts. Chem. Soc. Rev. 2016, 45, 2900−2936.
3. Jones, W. D. The Effects of Ancillary Ligands on Metal−Carbon Bond Strengths as Determined by C−H Activation. Top. Organomet. Chem. 2016, 56, 67−89.
4. Wang, Y.; Kuang, Y.; Wang, Y. $Rh_2(esp)^2$-Catalyzed Allylic and Benzylic Oxidations. Chem. Commun. 2015, 51, 5852−5855.
5. Dana, S.; Yadav, M. R.; Sahoo, A. K. Ruthenium-Catalyzed C−N and C−O Bond-Forming Processes from C−H Bond Functionalization. In C-H Bond Activation and Catalytic Functionalization; Springer, 2015; Vol. 55, pp 189−215.

6. Bordeaux, M.; Galarneau, A.; Drone, J. Catalytic, Mild, and selective Oxyfunctionalization of Liner Alkanes: Current Challenges. Angew. Chem., Int. Ed. 2012, 51, 10712−10723.
7. Neetha, M.; Saranya, S.; Harry, N. A.; Anilkumar, G. Recent Advances, and Perspectives in the Copper-Catalysed Amination of Aryl and Heteroaryl Halides. ChemistrySelect 2020, 5, 736−753.
8. Li, P.; Wang, Y.; Wang, X.; Wang, Y.; Liu, Y.; Huang, K.; Hu, J.; Duan, L.; Hu, C.; Liu, J. Selective Oxidation of Benzylic C−H Bonds Catalyzed by Cu(II)/ {PMo12}. J. Org. Chem. 2020, 85, 3101−3109.
9. Modern Organocopper Chemistry; Krause, N., Ed.; Wiley-VCH: Weinheim, Germany, 2002. https://onlinelibrary.wiley.com/doi/book/10.1002/3527600086
10. Niveditha, C. V.; Fatima, M. J. J.; Sindhu, S. Comprehensive Interfacial Study of Potentia-Dynamically Synthesized Copper Oxide Thin Films for Photoelectrochemical Applications. J. Electrochem. Soc. 2016, 163, H426−H433.

Chapter 3 Cu_2O Nanocrystals for Facet Selective Benzylic C_{sp3}-H Bond Oxidation: (100) Facets are not always Inactive

The study of the fate of oxidation reactions on the other facets of lower Millar indices like (001), (101), (110), etc. of Cu_2O nanocrystals was studied in chapter 3. Through this study, we explored the basic question, why do some facets show more photocatalytic activity towards some organic substrates resulting in photodegradation and some remain inactive at all? Do the organic reaction mechanism pathways (ionic or free radical) decide the catalyst's facets selectivity?

Methodology

For Synthesis of c- and *d*-Cu_2O NCs 223 mL and 173 mL of DI water were taken in two separate RBFs, which were placed in a water bath at 32-34°C. Then 12.5 mL of 0.1M $CuCl_2$

solution and 2.175g SDS were added to each RBF with vigorous stirring. After complete dissolution of SDS, 4.5 mL of 1.0M NaOH solution was introduced, each. Finally, 10 mL (for Cc) and 60 mL (for Dh) of 0.1M $NH_2OH.HCl$ was quickly injected. The solutions were kept in a water bath for 1 h for the growth of nanocrystals and centrifuged at 5000 rpm for 3 min. The precipitates were washed several times to ensure the removal of any organic impurities two times with DI water and finally with absolute alcohol. Samples were dried overnight at 50 °C in the vacuum oven Cu_2O nanocrystals (NCs) with different morphologies have been synthesized by wet chemical methods. By powder X-ray diffraction (PXRD), field emission scanning electron microscopy (FESEM), and high-resolution transmission electron microscopy (HRTEM), it was confirmed that the synthesized material was Cu_2O NCs with octahedral (Oh), dodecahedral (Dh) and cubic (Cc) morphologies with (111), (110), and (100) facets exposed, respectively. The synthesized Cu_2O NCs with the above morphologies have been explored as the catalyst for benzylic C_{sp3}-H bond oxidation. For this purpose, a model reaction of oxidation of diphenylmethane (DPM) by using t-butyl hydroperoxide (TBHP) as an oxidant at RT was carried out in an acetonitrile medium.

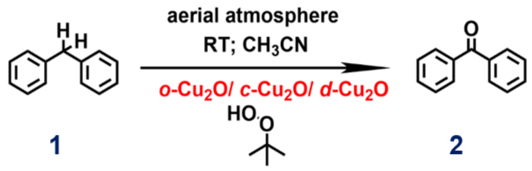

Out of all the morphologies evaluated, Cc Cu_2O NCs show the highest activity. The model oxidation reaction was completed within 3 days with ~99% yield and 100% selectivity for benzophenone as a sole product in the presence of c-Cu_2O NCs without any catalyst annihilation.

Sr. No.	Morphology	Major surfaces exposed for catalysis	Reaction time (time required to complete the reaction) (days)	Yield [a] (at the end of the reaction) (%)	Observations
1	c-Cu_2O	{100}	3 (3)	98 (99)	**No leaching/valorization of the catalyst**
2	o-Cu_2O	{111}	3 (5)	80 (92)	Complete catalyst valorization
3	d-Cu_2O	{110}	3 (4)	88 (92)	Partial catalyst valorization in the stipulated time period

Conclusions

(100), (111), and (110) faceted Cu_2O NCs having Cc, Oh, and Dh morphologies, respectively have been synthesized and characterized. The exposed facets of Cu_2O NCs were explored as catalytic sites for the benzylic sp^3C-H bond oxidation process under the optimized reaction conditions from the previous work. in the case of Cu^{1+} ended (111) facets of *o*-Cu_2O NCs are capable to activate oxygen molecules to undergo reduction by the SET mechanism in presence of light, and the in situ generated superoxo species immediately abstract the ·H radical from the nearby substrate and initiate the cascade of chemical reactions and electronic processes resulting into stable oxidation product and complete restructuring of the crystal lattice of the catalyst, respectively while (100) surfaces of c-Cu_2O NCs seems to be activated for the processes where surface generated excitons transfer through band-gap are not required resulting into the desired oxidation product instead of complete degradation of the substrate and these processes become predominant when TBHP like mild oxidant (which can produce ·O-Bu^t like stable free radicals) present in the vicinity.

Suggestions/ Recommendations

It can be claimed that oxygen-ended c-Cu_2O (100) surfaces are inactive for photophysical and photochemical processes like dye degradation. But these {100} surface planes are highly active for metal oxide semiconductor-based oxidation processes. Oxygen-ended (100) facets of cubic Cu_2O NCs can do the oxidation process faster than any other facet.

Bibliography/ Webliography

1. Zhou, K.; Wang, X.; Sun, X.; Peng, Q.; Li, Y. Enhanced catalytic activity of ceria nanorods from well-defined reactive crystal planes. *J. Catal.* **2005**, *229*, 206–212.
2. Tan, C. -H.; Hsu, S. –C.; Ke, W. –H.; Chen, L. –J.; Huang, M. H. Facet-Dependent Electrical Conductivity Properties of Cu_2O Crystals. *Nano Lett.* **2015**, *15*, 2155–2160.
3. Huang, W.-C.; Lyu, L.-M.; Yang, Y.-C.; Huang, M. H. Synthesis of Cu_2O Nanocrystals from Cubic to Rhombic Dodecahedral Structures and Their Comparative Photocatalytic Activity. *J. Am. Chem. Soc.* **2012**, *134*, 1261–1267.
4. Huang, M. H.; Naresh, G.; Chen, H. –S. Facet-Dependent Electrical, Photocatalytic, and Optical Properties of Semiconductor Crystals and Their Implications for Applications, *ACS Appl. Mater. Interfaces* **2018**, *10*, 4–15.
5. Shang, Y.; Guo, L. Facet-Controlled Synthetic Strategy of Cu_2O-Based Crystals for Catalysis and Sensing. *Adv. Sci.* **2015**, *2*, 1500140.
6. Bai, S.; Wang, L.; Li, Z.; Xiong, Y. Facet-Engineered Surface and Interface Design of Photocatalytic Materials. *Adv. Sci*. **2017**, *4*, 1600216.
7. Hua, Q.; Cao, T.; Bao, H.; Jiang, Z.; Huang, W. Crystal-Plane-Controlled Surface Chemistry and Catalytic Performance of Surfactant-Free Cu_2O Nanocrystals. *ChemSusChem* **2013**, *6*, 1966 – 1972.
8. Ho, J.-Y.; Huang, M. H. Synthesis of Submicrometer-Sized Cu_2O Crystals with Morphological Evolution from Cubic to Hexapod Structures and Their Comparative Photocatalytic Activity. *J. Phys. Chem. C* **2009**, *113*, 14159–14164.
9. Fine Chemicals through Heterogeneous Catalysis; Sheldon, R. A.; van Bekkum, H., Ed.; Wiley-VCH: Verlag CimbH, 2001. https://www.wiley.com/en-us/Fine+Chemicals+through+Heterogeneous+Catalysis-p-9783527612970
10. Liquid Phase Aerobic Oxidation Catalysis: Industrial Applications and Academic Perspectives; Stalh, S. S.; Alsters, P. L., Ed.; Wiley-VCH, Weinheim, 2016. https://www.wiley.com/ensg/Liquid+Phase+Aerobic+Oxidation+Catalysis:+Industrial+Applications+and+Academic+Perspectives-p-9783527690121

Chapter4 Synthesis and characterization of Fe, Ni (dual Metal-Metal) doped ZnS NPs and their photocatalytic activity

Methodology

In this study, Fe, Ni mono, and co-doped (metal/metal) ZnS Nps at 5.0% and 7.0% concentrations have been synthesized by the wet chemical method. PXRD confirmed that as-synthesized Nps were in the cubic phase while in $Zn_{1-0.14}Fe_{0.07}Ni_{0.07}S$ and $Zn_{1-0.07}Fe_{0.07}S$ a phase transfer has been observed from cubic to wurtzite.

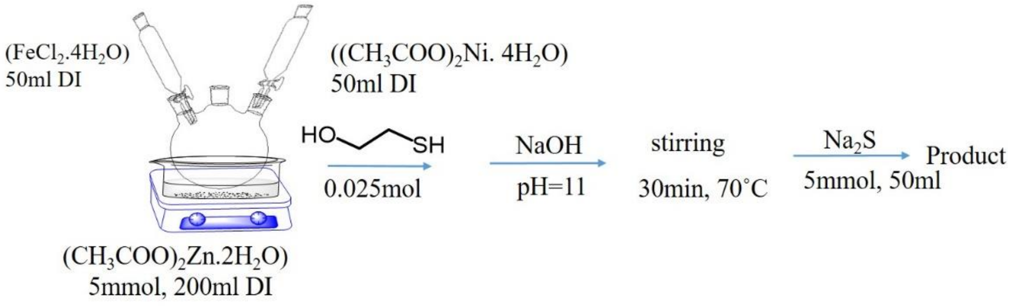

Fig: Catalyst preparation scheme

Energy dispersive analyses were carried out to confirm the dopants. Furthermore, the optical study, VSM analyses, HRTEM, BET surface area analyses, and electrochemical analyses were carried out to know the electronic structures of the as-synthesized NPS. The synthesized NPs were evaluated for the photocatalytic activity of rhodamine B dye degradation under the HMPV lamp. The Density Functional Theory study was also performed to know the role of transition metal (TM) and non-metal interaction in terms of pπ-dπ coupling over rapid charge migration, reduced rate of recombination, increased optical absorbance, and formation of charge trapping sites boosts photocatalytic efficiency exponentially.

Conclusion

The presence of transition metal induces ferromagnetic properties leading to its utilization as a reusable photocatalyst increasing its life cycle for better dye degradation and water-splitting ability. Theoretical study on Fe, Ni mono, co-doped ZnS system provides an explanation by highlighting band edge straddling, large variance in the effective mass of photo-generated electron-hole pair, and presence of intermediate states in the trapping reducing the recovery time to enhance reaction activity over the free surface of ZnS. The highest photocatalytic activity towards dye degradation was achieved in 5.33h by using $Zn_{1-0.10}Fe_{0.05}Ni_{0.05}S$ NPS.

Suggestions/ Recommendations

Pristine, mono-doped, and dual-doped ZnS NPs at different amounts of Fe and Ni (5.0%, 7.0% by wt) were synthesized and characterized. The XRD patterns suggest that at 7.0 % dopant concentration the phase of ZnS changes from cubic to hexagonal wurtzite. Inducing co-dopants in a material, synergistically enhance the efficiency of the catalyst. 5.0% Fe, Ni co-doped ZnS NPs show optimum photocatalytic activity due to

1. maximum surface stabilization due to charge distribution.
2. The distribution of dopant ions in Fe^{2+} and Fe^{3+} with Ni^{+2} and Ni^{+3}states plays an important role.
3. S atom acts as an efficient bridge forming a charge transfer channel between TM, and activates the whole surface.

Bibliography/ webliography

1. Torres-Martínez, C.L.; Kho, R.; Mian, O.I.; Mehra, R.K. Efficient photocatalytic degradation of environmental pollutants with mass-produced ZnS nano-crystals. *J. Colloid Interface Sci*. **2001** 240, 525–532.

2. Beydoun, D.; Amal, R.; Low, G.; McEvoy, S. *J. Nanoparticle Res*. **1999,** 439–458.

3. Ferreira, K.N.; Iverson, T.M.; Maghlaoui, K.; Barber, J.; Iwata, S. Architecture of the photosynthetic oxygen-evolving. *Center. Science.* **2004**, 303, 1831– 1838.

4. Fukuzumi, S.; Ohkubo, K. ; Suenobu, T. Long-lived charge separation and applications in artificial photosynthesis. *Acc. Chem. Res.* **2014**, 47 1455– 1464.

5. Pouretedal, H.R.; Norozi, A.; Keshavarz, M.H.; Semnani, A. Nanoparticles of zinc sulfide doped with manganese, nickel and copper as nanophotocatalyst in the degradation of organic dyes. *J. Hazard. Mater.* **2009**, 162, 674–681.

6. Aarthi, T.; Narahari, P.; Madras, G. Photocatalytic degradation of Azure and Sudan dyes using nano TiO_2. *J. Hazard. Mater.* **2007,** 149, 725–734.

7. Fu, H.; Pan, C.; Yao, W.; Zhu, Y. Visible-light-induced degradation of rhodamine B by nanosized Bi_2WO_6. *J. Phys. Chem. B* **2005,** 109, 22432–22439.

Chapter5 Synthesis and characterization of Fe, B (dual Metal-Non-Metal) doped ZnS NPs and their photocatalytic activity.

Methodology

In this chapter Fe, B mono, and co-doped (metal/metal) ZnS Nps at 5.0% and 7.0% concentrations have been synthesized by the wet chemical method. From PXRD it was confirmed that as-synthesized Nps were in the cubic phase while in $Zn_{1-0.14}Fe_{0.07}B_{0.07}S$ and $Zn_{1-0.07}Fe_{0.07}S$ a phase transfer has been observed from cubic to wurtzite.

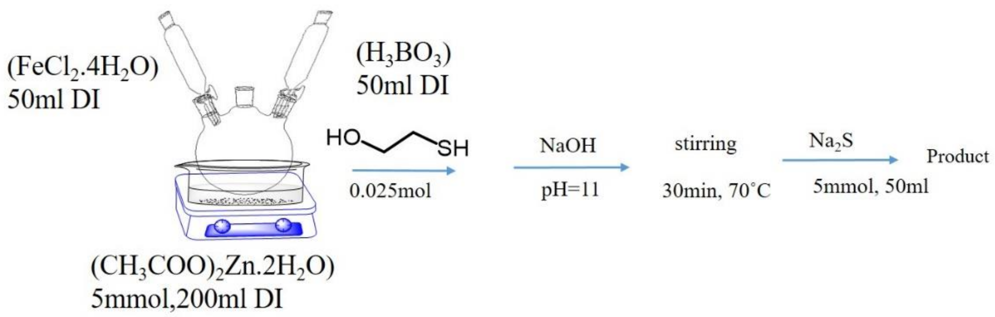

Fig: catalyst preparation scheme

Energy dispersive analyses were carried out to confirm the dopants. Furthermore, the optical study, VSM analyses, HRTEM, BET surface area analyses, and electrochemical analyses were carried out to know the electronic structures of the as-synthesized NPS. The synthesized NPs were evaluated for the photocatalytic activity of rhodamine B dye degradation under the HMPV lamp.

Conclusion

Pristine, monodoped, and co-doped ZnS NPs at different amounts of Fe and B (5.0%, 7.0% by wt) were synthesized and characterized. The XRD patterns suggest that at 7.0 % dopant concentration in both mono and co-doping, the phase of ZnS changes from cubic to hexagonal wurtzite. Inducing co-dopants in a material, synergistically enhance the efficiency of the catalyst to make the aqueous solution colorless.

Suggestions/ Recommendations

At 5.0% Fe, B co-doped ZnS NPs show optimum photocatalytic activity due to

1. Maximum surface stabilization due to charge distribution.
2. As the amount of co-dopant ions increases from 5.0 to 7.0%, photocatalytic efficiency decreases.

Bibliography/Webliography

1. Mahmood, Q.; Hassan, M.; Noor, N.A. Theoretical Study of Electronic, Magnetic, and Optical Response of Fe-doped ZnS: First-Principle Approach. *Journal of Superconductivity and Novel Magnetism*, **2017**, *30*, 1463-1471.
2. Momin, M.A.; Islam, M.A.; Majumdar, A.; Influence on structural, electronic and optical properties of Fe doped ZnS quantum dot: A density functional theory based study. *International Journal of Quantum Chemistry*, **2021**, 121, 26786.
3. Wan, H.; Xu, L.; Huang, W.Q.; Huang, G.F.; He, C.N.; Zhou, J.H; Peng, P.; Band engineering of ZnS by codoping for visible-light photocatalysis. *Applied Physics A.* **2014** 116, 741-750.
4. Hommel, D.; Hartmann, H.; Busse, W.; Gumlich, H.E.; Kreissl, J.; II–VI compounds codoped with transition metals and rare earths: ZnS: Mn^{2+} Sm^{3+} bulk crystals site selection and energy transfer. *Journal of luminescence*, **1991**, *48*, 655-660.

5. Li, D.F.; Luo, M.; Li, B.L.; Wu, C.B.; Deng, B.; Dong, H.N.; Low-resistivity p-type doping in wurtzite ZnS using codoping method. *Advances in Condensed Matter Physics, 2013*.

6. Hohenberg, P.; Kohn, W. Inhomogeneous electron gas. *Physical review*. 1964, *136*, 864.

7. Kohn, W.; Sham, L.J.; Self-consistent equations including exchange and correlation effects. *Physical review*.1965. *140*, 1133.